



Single-step modification of chitosan for toxic cations remediation from aqueous solution

Adnan Khan^{a,b,*}, Fazal Wahid^b, Nauman Ali^b, Syed Badshah^c, Claudio Airoidi^d

^aNational Centre of Excellence in Physical Chemistry, University of Peshawar, Peshawar, Khyber Pakhtunkhwa, Pakistan, Tel. +92 91 9216652; Fax: +92 91 9216652; email: adnanics@yahoo.com (A. Khan)

^bInstitute of Chemical Sciences, University of Peshawar, Peshawar, Khyber Pakhtunkhwa, Pakistan

^cDepartment of Chemistry, Gomal University, D. I. Khan, Khyber Pakhtunkhwa, Pakistan

^dInstitute of Chemistry, University of Campinas, UNICAMP, P.O. Box 6154, 13084-971 Campinas, SP, Brazil

Received 11 December 2013; Accepted 1 July 2014

ABSTRACT

Chitosan was chemically modified with 4-acryloylmorpholine in order to enhance Lewis basic centres in polymeric chain for cations removal. The new material was characterized using elemental analysis, infrared and ¹³C NMR in solid state and was applied for sorption of copper, lead and cadmium from aqueous solutions. The kinetic parameters were evaluated using pseudo-first- and second-order reaction. Kinetic results showed that the sorption process was best described by the pseudo-second-order model. The experimental data were adjusted to the Langmuir, the Freundlich and the Temkin sorption isotherms using both linear and nonlinear regression methods. The material showed the maximum sorption capacity for copper (3.35 mmol g⁻¹), than lead (1.60 mmol g⁻¹) and cadmium (0.74 mmol g⁻¹), obtained through the Langmuir sorption isotherm. The Langmuir model provided the lowest error values and fit better to the experimental data compared with other models.

Keywords: Chitosan; 4-acryloylmorpholine; Sorption; Langmuir; Cations

1. Introduction

Chitin is the second most abundant natural polymer after cellulose and can be extracted from fungi, insect, shrimp, lobster and krill. It is a linear polysaccharide, composed of randomly distributed β-(1→4) linked D-glucosamine and N-acetyl D-glucosamine [1,2]. Chitosan is obtained by alkaline deacetylation of chitin having unique characteristics such as biodegradability, biocompatibility, chemical inertness, nontoxic, high mechanical strength and low cost. It can be used for a variety of applications such as food packing,

separation membrane, drug delivery systems, biosensors and wastewater treatment. It has the ability to uptake several metal ions through different mechanisms, depends on the pH of the solution and the type of metal ion [3–5]. It is an attractive alternative to other conventional sorbents because of its low cost, availability, high reactivity and excellent chelating behavior [6–8].

Most of the heavy metals are toxic and carcinogenic agents such as lead, cadmium and excess of copper, when discharged in wastewater, becomes a serious threat to the human population [9]. Industrialization has accelerated the release of heavy metals into the environment. Important sources of heavy metals are

*Corresponding author.

mining industries, fertilizers, metal plating and fabrication, illegal landfills and abandoned waste disposal sites [10]. For heavy metal removal from liquid waste, a number of methods are used such as evaporation, electroplating, precipitation, ion exchange and membrane processes. However, these processes are not only expensive but also have a number of disadvantages such as incomplete metals removal, limited metal selectivity, very high or low working level of metals and toxic sludge production or other waste product that also need disposal [11,12]. Sorption is one of the most efficient techniques used for wastewater treatment. It is widely used because of its higher output, low cost and ability of removing trace metal ions from wastewater [13]. In the last decade, a growing interest has been shown towards chemical modification of chitosan and its derivatives in order to enhance their properties and consequently, expand their potential applications [14]. Besides the promising uses of chitosan, suitable alterations are essential to upturn the potential applications of this biomacromolecule. The amine and hydroxyl groups on each glucosamine repeating unit can act as reactive sites for chemical modification. Numerous attempts have been made for modification of chitosan either physically or chemically to improve its sorption capacity, pore size, mechanical strength, chemical stability, hydrophilicity and biocompatibility [15–17].

In the present study, chitosan was chemically modified through 4-acryloylmorpholine in order to improve its features as a sorbent in terms of its sorption capacity. The structure of chemically modified chitosan was confirmed using elemental analysis, FTIR and ^{13}C NMR spectroscopy. Thermal stability and morphology of chemically modified chitosan were determined using TG, Scanning electron microscopy (SEM) and X-ray diffraction techniques. Batch sorption experiments were carried out to observe the sorption capacity of copper, lead and cadmium onto chemically modified chitosan. The Langmuir, Freundlich and Temkin models were used to evaluate the sorption equilibrium data. Both linear and nonlinear regression techniques were applied to sorption study.

2. Experimental

2.1. Materials

Powdered chitosan, with 78% of degree of deacetylation, determined from infrared spectroscopy was obtained from crab extraction and supplied by Primex Ingredients AS (Norway), acryloylmorpholine (Aldrich), ethanol (Synth), cadmium (Merck), lead (Merck) and copper (Merck) nitrates were all of analytical grade and were used without purification.

2.2. Characterization

Elemental analysis was performed using Perkin Elmer model PE 2400 elemental analyzer. Bomem Spectrophotometer, MB-series, in the $4,000\text{--}400\text{ cm}^{-1}$ range, with 4 cm^{-1} of resolution, KBr pellets were used accumulating 32 scans. Solid-state ^{13}C NMR spectra of the samples were obtained using Bruker AC 300/P spectrometer with CP/MAS technique. The measurements were obtained at 75.47 MHz frequencies, with magic angle spinning of 4 kHz, pulse repetitions of 5 s and contact times of 1 ms. X-ray diffraction patterns were obtained on a Shimadzu XD-3A diffractometer (35 kv, 25 mA), in the 2θ form over the $1.5\text{--}50^\circ$ range with nickel-filtered $\text{CuK}\alpha$ radiation, with a wavelength of 0.154 nm. Thermogravimetric curves were obtained on a Shimadzu TGA 50 apparatus under argon atmosphere at a flow rate of $30\text{ cm}^3\text{ s}^{-1}$, with a heating rate of 0.167 K s^{-1} . SEM data were obtained from detection of the secondary electron images on a JEOL JSM 6360LV scanning electron microscope, operating at 20 kV. The samples were fixed onto a double-faced carbon tape adhered to a gold support and carbon coated in a Bal-Tec MD20 instrument. Cations sorbed were determined by comparing between the initial concentration in the aqueous solution and that found in supernatant using a Perkin Elmer 3000 DV ICP-OES apparatus. Each experimental point was performed in duplicate run.

2.3. Synthesis

Chitosan was chemically modified with 4-acryloylmorpholine in order to incorporate Lewis basic centres for cations removal. In a typical procedure, 3 g of chitosan (15 mmol) was suspended in 100 cm^3 of ethanol in a 250 cm^3 three-necked flask with stirring for 20 min at a temperature of 328 K. Then to this suspension, 3 cm^3 of 4-acryloylmorpholine (22.87 mmol) was slowly added in the presence of 1 cm^3 of triethylamine as a catalyst. The reaction mixture was stirred for further 24 h at 328 K. The product obtained was filtered, washed with water, ethanol and dried under vacuum at 318 K for 6 h. The proposed mechanism of reaction is shown in Fig. 1.

2.4. Sorption experiments

The sorption capacity of the new derivative for metal ions from aqueous solution was studied in duplicate runs using batch process. About 20 mg of the modified material was introduced into a series of polyethylene bottles, containing 25.0 cm^3 of cation

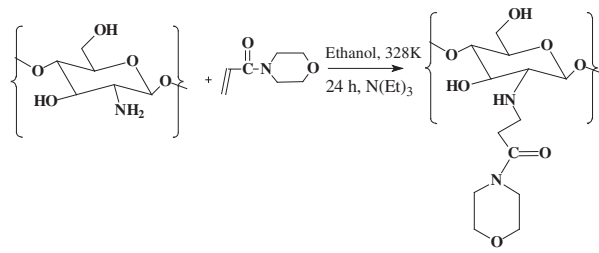


Fig. 1. Proposed reaction mechanism for synthesis of chemically modified Chitosan CHAM.

solutions with concentrations ranging from 7.0×10^{-4} to 2.0×10^{-3} mol dm⁻³. To obtain isothermal saturation, kinetic experiments were performed using these cation solutions. Sorption equilibrium was obtained at 4 h in an orbital apparatus at 298 ± 1 K near neutral pH. However, 6 h was chosen to ensure the best equilibrium conditions.

The supernatant solutions were separated from the solid through decantation and the amount of cations remaining in the aliquots was determined by ICP-OES. The amount of the cation sorbed in the experiment (mmol g⁻¹) was calculated using Eq. (1):

$$Nf = \frac{ni - ns}{m} \quad (1)$$

where Nf is the number of moles sorbed. While, ni and ns are the number of moles in the initial solution and in the supernatant after equilibrium and m is the mass of the sorbent used in each experiment [18]. Different isotherm equations have been used to know the equilibrium nature of sorption and the data were applied to the Langmuir, the Freundlich and the Temkin models.

2.5. Equilibrium isotherms

Sorption isotherms are important to know that how sorbates interact with sorbents and to optimize the use of sorbents. Thus, the correlation of equilibrium data either by theoretical or empirical equation is essential for practical design and operation of sorption system. In this study, three isothermal models: Langmuir, Freundlich and Temkin were used to evaluate experimental data.

2.5.1. Langmuir isotherm

The Langmuir isotherm suggests that the equilibrium is attained when a monolayer of sorbate saturates

the sorbent and whole sites have equal energies and enthalpies during sorption. [15]. The Langmuir isotherm model is expressed in Eq. (2):

$$\frac{Cs}{Nf} = \frac{Cs}{Ns} + \frac{1}{Nsb} \quad (2)$$

where Nf is the maximum sorption capacity at equilibrium, Cs is the equilibrium concentration, Ns and b are the Langmuir constants represent maximum sorption capacity and sorption energy, respectively [19–21]. For better comparison between linear and nonlinear regression techniques, four linear forms of the Langmuir model were applied to sorption study as shown in Table 1 [22].

2.5.2. The Freundlich isotherm

The Freundlich isotherm is the earliest known relationship, describes the surface heterogeneity, the exponential distribution of active sites and their energies. This isotherm suggests multilayer sorption on the surface of sorbent [23,24].

The Freundlich isotherm is expressed by the following equations:

$$Nf = K_f Cs^{\frac{1}{n}} \quad (3)$$

$$\log Nf = \log K_f + \frac{1}{n} \log Cs \quad (4)$$

where K_f and n are constants that show sorption capacity and sorption intensity of the sorbent. The plot of $\log Nf$ vs. $\log Cs$ for the sorption is used to generate K_f and n from the intercept and the slope values, respectively.

2.5.3. Temkin isotherm

Temkin and Pyzhev developed this isotherm and suggested that the heat of sorption would decrease linearly with the increase of coverage of sorbent [25]. The Temkin isotherm has been used in the following form:

$$Nf = \ln (K_T Cs)^{\frac{1}{n_T}} \quad (5)$$

$$Nf = n_T \ln K_T + n_T \ln Cs \quad (6)$$

Table 1
Langmuir Isotherm and their linear and nonlinear forms

Isotherm	Nonlinear form	Linear form	Plot
Langmuir type 1	$Nf = \frac{NsbCs}{1 + bCs}$	$\frac{Cs}{Nf} = \frac{Cs}{Ns} + \frac{1}{Nsb}$	$\frac{Cs}{Nf} Vs Cs$
Langmuir type 2		$\frac{1}{Nf} = \left(\frac{1}{Nsb}\right) \frac{1}{Cs} + \frac{1}{Ns}$	$\frac{1}{Nf} Vs \frac{1}{Cs}$
Langmuir type 3		$Nf = Ns - \left(\frac{1}{b}\right) + \frac{Nf}{Cs}$	$Nf Vs \frac{Nf}{Cs}$
Langmuir type 4		$\frac{Nf}{Cs} = bNs - bNf$	$\frac{Nf}{Cs} Vs Nf$

A plot of $\ln Cs$ vs. Nf gives us K_T , n_T and b values. The constant b is heat of sorption, and can be calculated from the following equation:

$$n_T = \frac{RT}{b} \quad (7)$$

To evaluate the fitness of the isotherm equation to the experimental equilibrium data, an error function is required to enable the optimization procedure. Three parameters: the chi-square (χ^2), the standard error (SE) and correlation coefficient (R) of the estimated values were used to determine the validity of each model. The mathematical equations that represent the SE and chi-square are shown in Eqs. (8) and (9):

$$SE = \sqrt{\frac{1}{m-P} \sum_{i=1}^m (Nf_{\text{exp}}^i - Nf_{\text{cali}})^2} \quad (8)$$

$$\chi^2 = \sum_{i=1}^m \frac{(Nf_{\text{exp}}^i - Nf_{\text{cali}})^2}{Nf_{\text{cali}}} \quad (9)$$

where Nf_{exp} is the number of moles sorbed experimentally while Nf_{cali} is the number of moles calculated from each model. The number of points present in each isotherm is m and P is the number of parameters in each equation [26,27].

3. Results and discussion

Chitosan was chemically modified through a single-step reaction based on aza Michael reaction. The reaction was carried out in ethanol in which acrylamide acts as a Michael acceptor. This is a new procedure for the modification of chitosan in which a pendant chain is directly bonded to the amino group of the biopolymer, as shown in Fig. 1. The basic centres attached to pendant chain were used for cations removal.

3.1. Elemental analysis

For chitosan (CH) and chemically modified chitosan carbon, nitrogen elemental analysis and C/N relationship are summarized in Table 2. The general amount of each element (L_0) attached in the pendant chains is calculated using the expression 10. It is clear from Table 2 that the number of moles of carbon and nitrogen in chemically modified chitosan increased when compared with precursor chitosan. An increase in the moles of carbon is high as compared with nitrogen because acryloylmorpholine molecule contains more carbons than nitrogen. These values reflect the incorporation of acryloylmorpholine moiety as a pendant chain in the precursor chitosan.

$$L_0 = \frac{\% \text{Element} \times 10}{\text{Atomic mass of element}} \quad (10)$$

3.2. Infrared spectroscopy

The FTIR spectrum of precursor chitosan (CH) contains characteristic bands associated with polymeric backbone, such as: (a) a large band at $3,400 \text{ cm}^{-1}$ is assigned to the OH stretching frequency which overlaps with amino stretching frequency in the same region; (b) typical C–H stretching vibrations bands at $2,916$ and $2,877 \text{ cm}^{-1}$; (c) the absorption band at

Table 2
Percentages of carbon (C) and nitrogen (N), number of moles for chitosan (CH) and chemically modified chitosans (CHAM) and the corresponding molar ratio (C/N)

Sample	C/%	N/%	C/mmolg ⁻¹	N/mmolg ⁻¹	C/N
CH	40.63	7.39	33.86	5.27	6.42
CHAM	41.99	7.67	34.99	5.48	6.38

1,655 cm^{-1} is assigned to amide I; (d) the band at 1,597 cm^{-1} is attributed to N–H bond; (e) the sharp bands at 1,379 and 1,419 cm^{-1} represent C=O and CH_3 deformation mode of acetamide groups, remaining from chitin, due to its incomplete deacetylation and the broad band at 1,076 cm^{-1} indicates the presence of C–O stretching vibration [28].

The spectrum of chemically modified biopolymer showed some spectral changes as shown in Fig. 2. The bands for amide I and N–H have increased in intensity and have become larger due to increased number of carbon–nitrogen bonds between acryloylmorpholine and chitosan. These changes confirm the proposed chemical modification.

3.3. Nuclear magnetic resonance

The ^{13}C NMR spectra in the solid state for pristine chitosan (CH) and chemically modified (CHAM) chitosan are shown in Fig. 3. For the chitosan spectrum, a set of five distinct peaks were present and assigned to C1, C2, C4, C6 and C3/C5 at 105, 57, 84, 62 and 75 ppm, respectively. In addition, two other signals at 19 and 175 ppm are attributed to methyl and the carbonyl carbon associated with the monomeric form remaining from chitin due to the incomplete deacetylation of the original biopolymer [29]. As expected, the chemically modified chitosan (CHAM) presented peaks at 57 and 62 ppm for C2 and C6 that are well separated due to the increased number of carbon–nitrogen bonds. The peak at C2 position due to carbon–nitrogen bond and peak at 175 ppm corresponding amide group also increased in intensity

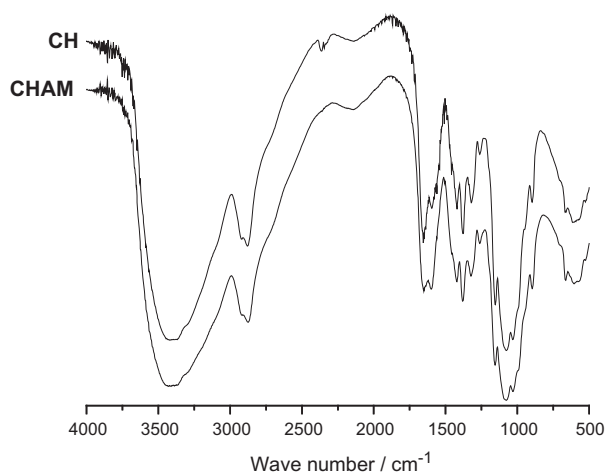


Fig. 2. Infrared spectra of chitosan CH and chemically modified chitosan CHAM.

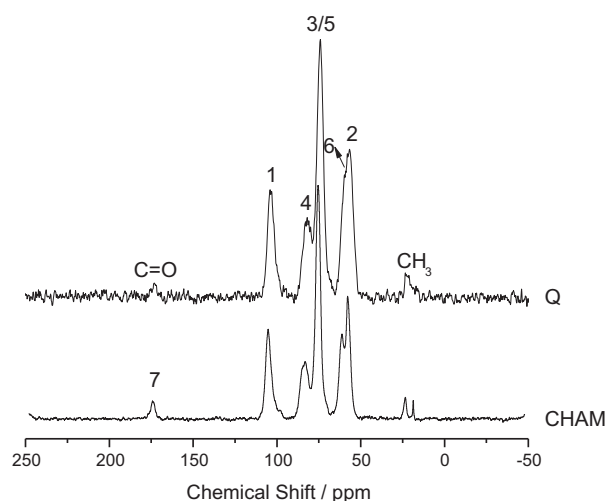


Fig. 3. ^{13}C NMR spectra in solid state of chitosan CH and chemically modified chitosan CHAM.

further confirms the successful chemical modification of the precursor chitosan.

3.4. X-ray diffraction

The X-ray analysis was conducted to find out the effect of the chemical modification upon the crystallinity of the precursor chitosan. Pure chitosan presents a diffraction pattern that indicates poor crystallinity, as can be seen through the two characteristic broad peaks at $2\theta = 9^\circ$ and $2\theta = 18^\circ$ as shown in Fig. 4. For

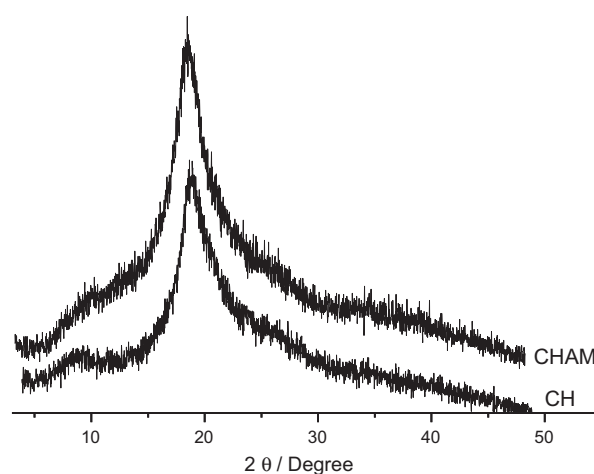


Fig. 4. X-ray diffractogram patterns for chitosan CH and chemically modified chitosan CHAM.

chemically modified biopolymer (CHAM), the first peak disappear completely and the second peak appears at the same value $2\theta = 18^\circ$ as for original chitosan. After pendant chain incorporation on the polymeric backbone, only the peak at 20° was observed. This means that there is a further decrease in the crystallinity of the chemically modified chitosan with respect to the precursor biopolymer. This behavior occurs due to entry of new molecule inside the two polymeric chains that lead to disruption of intermolecular hydrogen bonds in the structure of chitosan. The present results corroborate those obtained using infrared and nuclear magnetic resonance spectroscopy that confirms the chemical modification of the precursor chitosan [30].

3.5. Thermogravimetry

Thermal analysis of precursor chitosan (CH) and chemically modified chitosan (CHAM) was carried out in order to determine the effect of chemical modification on thermal stability of the sorbent. The TG and DTG curves of precursor chitosan (CH) clearly show two events as observed in Fig. 5. The first stage of decomposition occurred at 335 K with a mass loss of 9%, which was mainly due to the loss of physically sorbed water on material surface and the second peak at 570 K with a mass loss of 57% due to the biopolymer decomposition [31], as shown in Fig. 5. For chemically modified chitosan (CHAM), slightly lower value of the first and second decomposition stages was observed compared with precursor chitosan, indicating a moderate degree of functionalization. The derivative profile for chemically modified chitosan showed the first peak

due to water loss appear at 331 K with a mass loss of 11% and the second peak appear at 565 K with a mass loss of 50% due to the biopolymer decomposition as shown in Fig. 6. The temperature of the second stage of decomposition for chemically modified chitosan is lower, however, the small loss of mass occurred at this stage compared with precursor chitosan showing more thermal stability due to modification, highlighting a structural difference between them.

3.6. Scanning electron microscopy

The SEM images of original chitosan (CH) and chemically modified chitosan (CHAM) are shown in Fig. 7. The precursor chitosan has a smooth fluffy surface with wrinkles and somewhat folding microstructure. But in case of chemically modified chitosan, an entirely different morphological structure emerged and the sorbent surface was aligned with a non-uniform and irregular way to form many ridges as shown in Fig. 7.

3.7. Sorption study

Important information such as how the sorbate molecules are distributed between the liquid/solid phase in the equilibrium state can be interpreted from sorption isotherms. The sorption capacity of modified chitosan was higher for copper than that of lead and cadmium as shown in Table 3. It is to be noted that the higher sorption capacity for copper is due to Hard/Soft acid–base interactions [32]. Nitrogen is a border line Lewis basic centre and copper is also a borderline metal, as a result, chemically modified chitosan

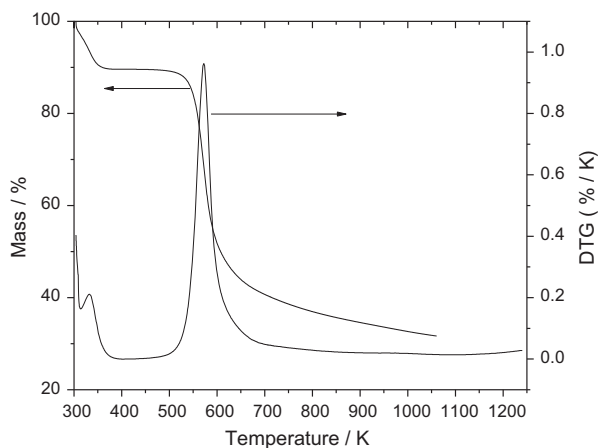


Fig. 5. Thermogravimetric and derivative curves for chitosan CH.

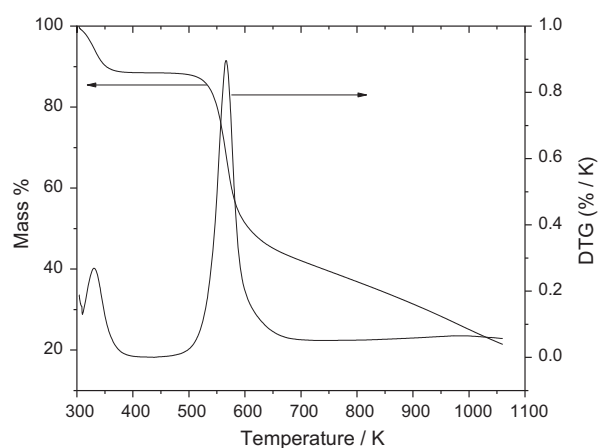


Fig. 6. Thermogravimetric and derivative curves for chemically modified chitosan CHAM.

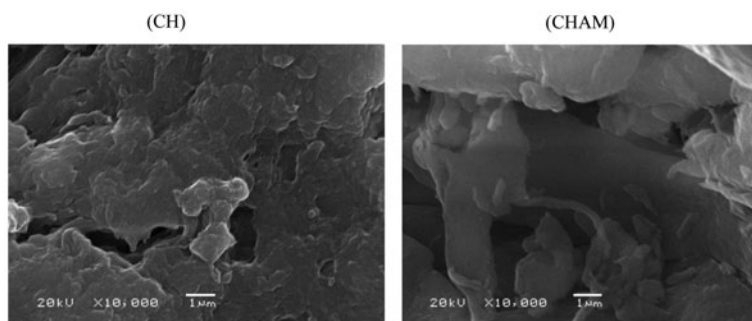


Fig. 7. SEM images of chitosan CH and chemically modified chitosan CHAM.

Table 3

Number of moles sorbed (N_f), parameters of the Langmuir (N_s and b), correlation coefficients (r) and SEs for the interaction of divalent metals with modified chitosan CHAM, at 298 ± 1 K using linear method

Material	Isotherm	Constant	Type I	Type II	Type III	Type IV
CHAM	Cu^{2+}	N_f (mmol g^{-1})	3.35	3.35	3.35	3.35
		N_s (mmol g^{-1})	3.55 ± 0.01	3.21 ± 0.01	3.38 ± 0.09	3.43 ± 0.61
		b (g mmol^{-1})	1.94 ± 0.004	3.51 ± 0.002	3.03 ± 0.02	2.89 ± 0.22
		R^2	0.997	0.989	0.946	0.946
		SE	0.22	0.36	0.17	0.11
	Pb^{2+}	N_f (mmol g^{-1})	1.60	1.60	1.60	1.60
		N_s (mmol g^{-1})	1.81 ± 0.11	1.62 ± 0.05	1.79 ± 0.08	1.84 ± 0.04
		b (g mmol^{-1})	0.42 ± 0.01	0.52 ± 0.05	0.43 ± 0.21	0.40 ± 0.03
		R^2	0.996	0.984	0.934	0.934
		SE	0.16	0.11	0.08	0.05
	Cd^{2+}	N_f (mmol g^{-1})	0.74	0.74	0.74	0.74
		N_s (mmol g^{-1})	0.77 ± 0.07	0.77 ± 0.01	0.77 ± 0.007	0.77 ± 0.04
		b (g mmol^{-1})	1.62 ± 0.02	1.76 ± 0.02	1.73 ± 0.02	1.71 ± 0.06
		R^2	0.999	0.992	0.985	0.985
		SE	0.01	0.01	0.01	0.01
	χ^2	0.001	0.001	0.001	0.001	

showed higher sorption capacity for copper (3.35 mmol g^{-1}) than lead (1.60 mmol g^{-1}) and cadmium (0.74 mmol g^{-1}) as shown in Fig. 8. The modified chitosan showed higher sorption than precursor chitosan for copper 1.60 and lead 1.19 mmol g^{-1} . These values are higher when compared with raw chitosan as shown in Table 3. However, it is not easy to compare the values due to difference in chitosan source, the degree of deacetylation and also the form found [33]. However, the sorption capacity of chitosan was higher for lead 1.35 mmol g^{-1} than chemically modified chitosan. The order of sorption was $\text{Cu} > \text{Pb} > \text{Cd}$. The linear form of Langmuir sorption isotherm for the metals studied is shown in Fig. 9.

Different linear forms of Langmuir models gave different values of the constants and distribution of

errors as shown in Table 3. In case of copper and lead, the differences between constants are higher, when different linear forms of the Langmuir model were used. This difference in values may be due to different axial arrangements. However, in case of cadmium the value of constants is very close to each other, so it means that experimental factors also involved in different values of the constants. The lowest values of error were found for the Langmuir model type IV for the three metals. Error functions of Freundlich model were higher than Langmuir model showing that it does not fit better to experimental data, however, in case of Temkin model, the smallest value of the SE and chi-square test was found, which shows that this model fits better to experimental data than Langmuir and Freundlich model as shown in Table 4.

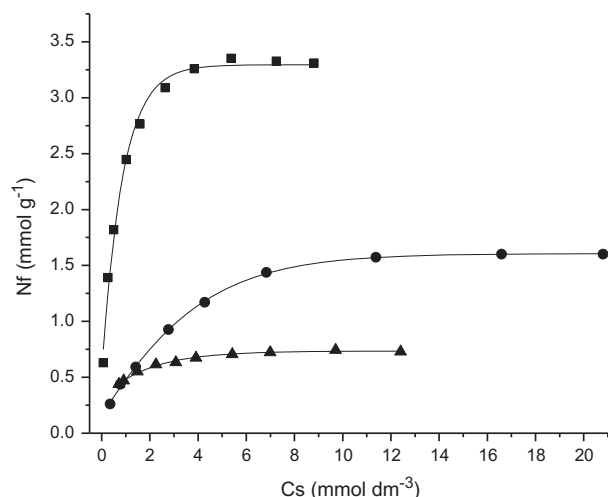


Fig. 8. Experimental sorption isotherm of chemically modified chitosan CHAM for (a) lead (▼), cadmium (●) and (b) copper (■) 298 ± 1 K.

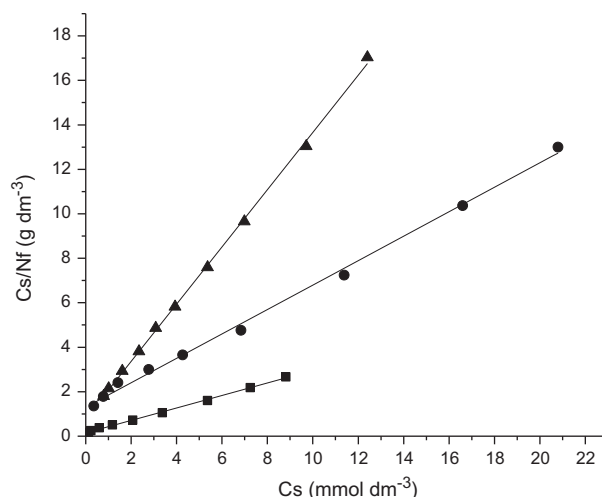


Fig. 9. Linear form of Langmuir sorption isotherm for copper (■), lead (●) and cadmium (▼).

The values of different error functions corresponding to the nonlinear Langmuir equation are smaller than those of the Freundlich and the Temkin models as shown in Table 5. Nonlinear regression analysis corresponds to the best way to select the isotherm that fits better to the experimental data. This method involves an attempt to minimize the distribution of errors between experimental data and the isotherm considered as shown in Fig. 10. Both linear and nonlinear regression analysis produces different models as the best fitting isotherm for the given set of data, thus indicating a significant difference between the analytical methods.

3.8. Kinetic study

Kinetics study enlightens the rate of uptake of cations on chemically modified chitosan and the time required to reach equilibrium. It can be observed that sorption of copper and cadmium achieved equilibrium within 3 h and maximum sorption capacity for copper reached to 3.35 mmol g⁻¹ as shown in Fig. 11. In case of lead, the sorption system achieve equilibrium within 4 h. The pseudo-first-order [34] and pseudo-second-order [35] were applied to predict the sorption kinetic process as shown in Eqs. (9) and (10).

$$\log(N_f - N_{ft}) = \log N_f - \left(\frac{k_1}{2.303} \right) t \quad (11)$$

Table 4

Number of moles sorbed (N_f), the Freundlich (n and K_f), the Temkin (b and K_T), Langmuir (N_s and b) parameters, correlation coefficient (r) and respective error for interaction of divalent metals with CHAM at 298 ± 1 K, using linear method

Method	Isotherm	Constant	Cu(II)	Pb(II)	Cd(II)
Linear	Freundlich	K_f (mmol g ⁻¹)	1.81 ± 0.01	0.51 ± 0.03	0.43 ± 0.01
		n	2.69 ± 0.02	2.18 ± 0.04	3.80 ± 0.01
		R^2	0.952	0.939	0.959
		SE	0.51	0.95	6.14
		χ^2	18.78	9.16	33.21
	Temkin	K_T (mmol dm ⁻³)	28.38 ± 0.06	4.74 ± 0.04	93.39 ± 0.01
		b (kJ mol ⁻¹)	1.596 ± 0.04	0.923 ± 0.04	0.272 ± 0.008
		R^2	0.962	0.966	0.958
		SE	0.217	0.09	0.02
		χ^2	0.26	0.08	0.008

Table 5

Number of moles sorbed (N_f), parameters of the Freundlich (n and K_f), Temkin (K_T and b), correlation coefficients (r) and respective error for interaction of Cu^{2+} , Pb^{2+} and Cd^{2+} with chitosan, CHAM at 298 ± 1 K, using nonlinear fit

Isotherm	Constant	Cu(II)	Pb(II)	Cd(II)
Langmuir	N_f (mmol g^{-1})		1.60	0.74
		3.35		
	N_s (mmol g^{-1})	3.64 ± 0.1	1.87 ± 0.05	0.77 ± 0.006
	b (g mmol^{-1})	1.61 ± 0.2	0.38 ± 0.03	1.69 ± 0.08
	R^2	0.984	0.990	0.991
	χ^2	0.02	0.003	0.0001
Freundlich	K_f (mmol g^{-1})	1.94 ± 0.13	0.61 ± 0.07	0.50 ± 0.01
	n	3.35 ± 0.45	2.83 ± 0.40	5.82 ± 0.65
	R^2	0.920	0.918	0.917
	χ^2	0.11	0.02	0.001
Temkin	K_T (mmol dm^{-3})	28.50 ± 7.28	4.74 ± 0.98	93.16 ± 43.50
	b (kJ mol^{-1})	1.55 ± 0.10	0.965 ± 0.17	0.295 ± 0.73
	R^2	0.966	0.970	0.950
	χ^2	0.04	0.009	0.006

where k_1 is the pseudo-first-order rate constant (min^{-1}) of sorption, N_f and N_{ft} (mmol/g) are the amounts of metal ion sorbed at equilibrium and time t (min), respectively. The N_f and k_1 are calculated by plotting the $\log(N_f - N_{ft})$ vs. t shows second-order sorption. The plot of $\log(N_f - N_{ft})$ vs. t for cadmium sorption on chemically modified chitosan is shown in Fig. 12.

The pseudo-second-order model can be written as follows:

$$\frac{t}{N_{ft}} = \frac{1}{K_2 N_f^2} + \left(\frac{1}{N_f}\right)t \quad (12)$$

where k_2 (g/mg min) is the second-order rate constant. The kinetic parameters for pseudo-second-order model are determined from the linear plots of (t/N_{ft}) vs. t . The calculated N_f values agree very well with experimental values and high value of the regression coefficient confirms that the sorption phenomena followed second-order kinetics. The first-order model provides a good fit to the experimental data, relative small error

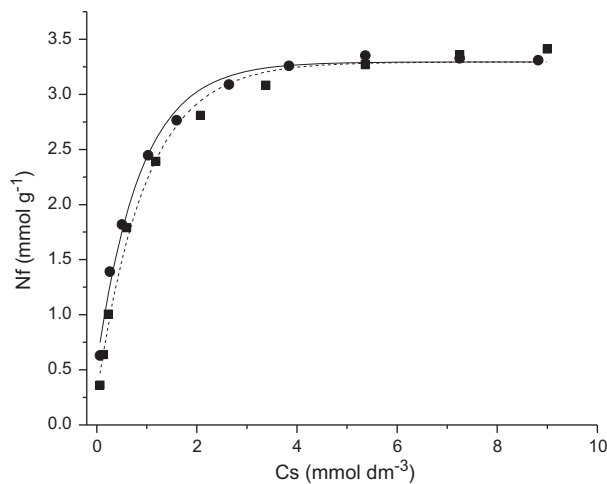


Fig. 10. Experimental (●) and nonlinear (■) Langmuir sorption isotherm for copper.

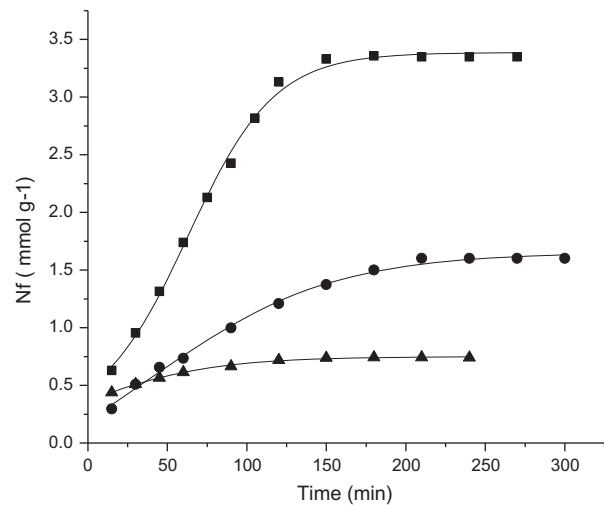


Fig. 11. Effect of contact time on cations sorption on chemically modified chitosan CHAM at 298 ± 1 K.

Table 6

Rate sorption constants for two kinetic models of chemically modified chitosan (CHAM) at 298 ± 1 K

Metal	First order			Second order		
	Nf (mmol g ⁻¹)	$K_1(10^{-2} \text{ min}^{-1})$	R^2	Nf (mmol g ⁻¹)	$K_2 (10^{-3} \text{ min}^{-1})$	R^2
Cu	7.14	2.58	0.890	4.63	2.34	0.967
Pb	1.88	1.46	0.956	2.46	3.29	0.966
Cd	0.63	2.93	0.938	0.79	78.9	0.998

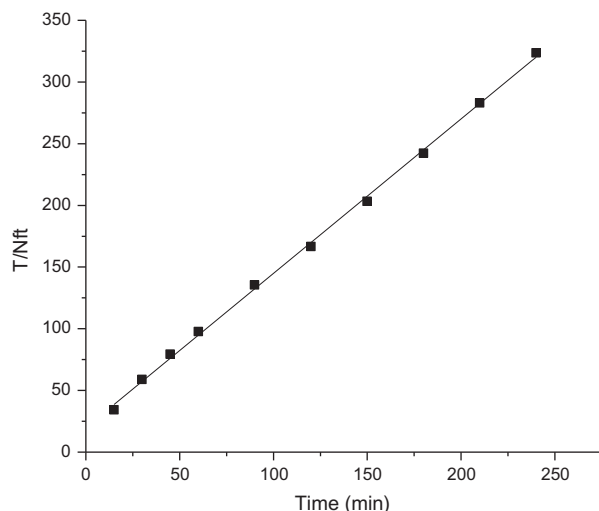


Fig. 12. Second-order plot for the sorption of cadmium on chemically modified chitosan CHAM.

value; however, the higher correlation coefficient (Table 6) of the second-order model indicated that the second-order model could better describe the sorption of copper, lead and cadmium on chemically modified chitosan. The value of Nf calculated from the pseudo-second-order equation is very close to experimental data. These values indicate a better fit of pseudo-second-order model with the experimental data as compared with the Lagergren first-order model. The pseudo-second-order rate expression described that the process is chemisorption involving valency forces through the sharing of electrons between the sorbent and sorbate as covalent forces.

4. Conclusion

The present work successfully described a single-step chemical modification of chitosan with acryloylmorpholine. Chemical modification of chitosan was confirmed by elemental analysis, FTIR and solid-state ¹³C NMR. Modified material presented promising removal of cations from aqueous solution. Based on

Langmuir sorption isotherm, modified chitosan sorption capacity was highest for copper as compared with lead and cadmium. This is due to the presence of a nitrogen, because both nitrogen and copper are the borderline Lewis base that has greater affinity for one another. The pseudo-second-order rate expression fits to experimental data, suggests that the rate-limiting step is chemisorption. The Temkin model, fits better to experimental data than the other two models.

Acknowledgements

The authors thank to FAPESP, TWAS-CNPq for financial support.

References

- [1] A.A.A. Emara, M.A. Tawab, M.A. El-ghamry, M.Z. Elsabee, Metal uptake by chitosan derivatives and structure studies of the polymer metal complexes, *Carbohydr. Polym.* 83 (2011) 192–202.
- [2] A.J.M. Al-Karawi, Z.H.J. Al-Qaisi, H.I. Abdullah, A.M.A. Al-Mokaram, D.T.A. Al-Heetimi, Synthesis, characterization of acrylamide grafted chitosan and its use in removal of copper(II) ions from water, *Carbohydr. Polym.* 83 (2011) 495–500.
- [3] A.G. Yavuz, A. Uygun, V.R. Bhethanabotla, Substituted polyaniline/chitosan composites: Synthesis and characterization, *Carbohydr. Polym.* 75 (2009) 448–453.
- [4] M. Monier, D.M. Ayad, Y. Wei, A.A. Sarhan, Adsorption of Cu(II), Co(II), and Ni(II) ions by modified magnetic chitosan chelating resin, *J. Hazard. Mater.* 177 (2010) 962–970.
- [5] L. Zhou, J. Liu, Z. Liu, Adsorption of platinum(IV) and palladium(II) from aqueous solution by thiourea-modified chitosan microspheres, *J. Hazard. Mater.* 172 (2009) 439–446.
- [6] D. Zeng, J. Wu, John F. Kennedy, Application of a chitosan flocculant to water treatment, *Carbohydr. Polym.* 71 (2008) 135–139.
- [7] Y.A. Aydın, N.D. Aksoy, Adsorption of chromium on chitosan: Optimization, kinetics and thermodynamics, *Chem. Eng. J.* 151 (2009) 188–194.
- [8] G. Crini, F. Gimbert, C. Robert, B. Martel, O. Adam, N. Morin-Crini, F. De Giorgi, P.M. Badot, The removal of Basic Blue 3 from aqueous solutions by chitosan-based adsorbent: Batch studies, *J. Hazard. Mater.* 153 (2008) 96–106.

- [9] M.A. Al-Ghouti, M.A.M. Khraisheh, M. Tutuji, Flow injection potentiometric stripping analysis for study of adsorption of heavy metal ions onto modified diatomite, *Chem. Eng. J.* 104 (2004) 83–91.
- [10] M.W. Wan, C. Kan, B.D. Rogel, M.L.P. Dalida, Adsorption of copper (II) and lead (II) ions from aqueous solution on chitosan-coated sand, *Carbohydr. Polym.* 80 (2010) 891–899.
- [11] N.G. Kandile, A.S. Nasr, Environment friendly modified chitosan hydrogels as a matrix for adsorption of metal ions, synthesis and characterization, *Carbohydr. Polym.* 78 (2009) 753–759.
- [12] D.D. Gang, B. Deng, L. Lin, As(III) removal using an iron-impregnated chitosan sorbent, *J. Hazard. Mater.* 182 (2010) 156–161.
- [13] A. Shafaei, F.Z. Ashtiani, T. Kaghazchi, Equilibrium studies of the sorption of Hg(II) ions onto chitosan, *Chem. Eng. J.* 133 (2007) 311–316.
- [14] I.M. El-Sherbiny, Synthesis, characterization and metal uptake capacity of a new carboxymethyl chitosan derivative, *Eur. Polym. J.* 45 (2009) 199–210.
- [15] W.S. Ngah, A. Kamari, S. Fatinathan, P. W. Ng, Adsorption of chromium from aqueous solution using chitosan beads, *Adsorption* 12 (2006) 249–257.
- [16] V.A. Vasnev, A.I. Tarasov, G.D. Markova, S.V. Vinogradova, O.G. Garkusha, Synthesis and properties of acylated chitin and chitosan derivatives, *Carbohydr. Polym.* 64 (2006) 184–189.
- [17] A. Kamari, W. Saime, W. Ngah, L.K. Liew, Chitosan and chemically modified chitosan beads for acid dyes sorption, *J. Environ. Sci.* 21 (2009) 296–302.
- [18] Y. Ho, W. Chiu, C. Wang, Regression analysis for the sorption isotherms of basic dyes on sugarcane dust, *Bioresour. Technol.* 96 (2005) 1285–1291.
- [19] M. Chabani, A. Amrane, A. Bensmaili, Equilibrium sorption isotherms for nitrate on resin Amberlite IRA 400, *J. Hazard. Mater.* 165 (2009) 27–33.
- [20] T.W. Weber, R.K. Chakravorti, Pore and solid diffusion models for fixed-bed adsorbents, *AIChE J.* 20 (1974) 228–238.
- [21] F.C. Wu, R.L. Tseng, R.S. Juang, A review and experimental verification of using chitosan and its derivatives as adsorbents for selected heavy metals, *J. Environ. Manage.* 91 (2010) 798–806.
- [22] S. Parimal, M. Prasad, U. Bhaskar, Prediction of equilibrium sorption isotherm: Comparison of linear and nonlinear methods, *Ind. Eng. Chem. Res.* 49 (2010) 2882–2888.
- [23] A.H. Chen, S.C. Liu, C.Y. Chen, C.Y. Chen, Comparative adsorption of Cu(II), Zn(II), and Pb(II) ions in aqueous solution on the crosslinked chitosan with epichlorohydrin, *J. Hazard. Mater.* 154 (2008) 184–191.
- [24] R. Donat, A. Akdogan, E. Erdem, H. Cetisli, Thermodynamics of Pb²⁺ and Ni²⁺ adsorption onto natural bentonite from aqueous solutions, *J. Colloid Interface Sci.* 286 (2005) 43–52.
- [25] S.J. Allen, G. Mckay, J.F. Porter, Adsorption isotherm models for basic dye adsorption by peat in single and binary component systems, *J. Colloid Interface Sci.* 280 (2004) 322–333.
- [26] K.S. Sousa, E.C. Silva Filho, C. Airoidi, Ethylenesulfide as a useful agent for incorporation into the biopolymer chitosan in a solvent-free reaction for use in cation removal, *Carbohydr. Res.* 344 (2009) 1716–1723.
- [27] S. Basha, Z.V.P. Murthy, B. Jha, Sorption of Hg(II) from aqueous solutions onto *Carica papaya*: Application of isotherms, *Ind. Eng. Chem. Res.* 47 (2008) 980–986.
- [28] A. Khan, S. Badshah, C. Airoidi, Biosorption of some toxic metal ions by chitosan modified with glycidylmethacrylate and diethylenetriamine, *Chem. Eng. J.* 171 (2011) 159–166.
- [29] A. Khan, S. Badshah, C. Airoidi, Dithiocarbamated chitosan as a potent biopolymer for toxic cation remediation, *Colloids Surf., B* 87 (2011) 88–95.
- [30] E.C.N. Lopes, K.S. Sousa, C. Airoidi, Chitosan–cyanuric chloride intermediary as a source to incorporate molecules—Thermodynamic data of copper/biopolymer interactions, *Thermochim. Acta* 483 (2008) 21–28.
- [31] D. Ono, J. Bragdon, D.A. Jaeger, Synthesis and characterization of dithiocarbamate surfactants, *Colloids Surf., A* 308 (2007) 141–146.
- [32] A. Alfara, E. Frackowiak, F. Béguin, The HSAB concept as a means to interpret the adsorption of metal ions onto activated carbons, *Appl. Surf. Sci.* 228 (2004) 84–92.
- [33] I.S. Lima, C. Airoidi, A thermodynamic investigation on chitosan-divalent cation interactions, *Thermochim. Acta* 421 (2004) 133–139.
- [34] S. Lagergren, Zur theorie der sogennanten adsorption geloster Stoffe (To the theory of so-called adsorption soluble substances), *K. Sven. Vetenskapskad. Handlingar* 24 (1898) 1–39.
- [35] Y.S. Ho, J. C.Y. Ng, Kinetics of pollutant sorption by biosorbents: Review, *Sep. Purif. Methods* 29 (2000) 189–232.